Journal of Power Sources 196 (2011) 6657–6662

Contents lists available at ScienceDirect

Journal of Power Sources

journal homepage: www.elsevier.com/locate/jpowsour

Silicon nanowires coated with copper layer as anode materials for lithium-ion batteries

Huixin Chen, Ying Xiao, Lin Wang, Yong Yang*

State Key Laboratory for Physical Chemistry of Solid Surfaces, College of Chemistry and Chemical Engineering, Department of Chemistry, Xiamen University, Xiamen, Fujian 361005, PR China

ARTICLE INFO

Article history:
Received 8 September 2010
Received in revised form
15 December 2010
Accepted 17 December 2010
Available online 7 January 2011

Keywords:
Silicon nanowires
Electrochemical performance
Lithium-ion batteries
Copper-coated

ABSTRACT

Silicon nanowires (Si NWs) with copper-coating as high capacity and improved cycle-life anode for lithium-ion batteries have been successfully prepared by chemical vapor deposition and magnetron sputtering methods. The morphology, structure, composition as well as the electrochemical performance of copper-coated Si NWs is characterized in detail. The results indicate that the copper-coated Si NWs electrodes show an initial coulombic efficiency of 90.3% when cycling between 0.02 V and 2.0 V (versus Li/Li^+) at a current density of 210 mA g^{-1}. The copper-coated Si NWs electrodes exhibit a capacity as high as 2700 mAh g^{-1} at the first cycle. They also show a good capacity retention and excellent rate capability compared with pristine and carbon-coated Si NWs.

1. Introduction

Lithium-ion batteries have been widely used for portable electronic devices and now also have a big potential application for electric vehicles and implantable medical devices. Exploring new electrode materials with high-energy capacity and long cycle life for lithium-ion batteries is one of the most important research topics in this field. Compared to the other anode materials, such as Al, Sn, etc., which are also able to make alloys with lithium, silicon is more attractive because it has the highest known theoretical specific mass capacity of 4200 mAh g^{-1} due to the incorporation of 4.4 lithium atoms for per silicon atom [1]. Moreover, considering future commercial applications, silicon is also very attractive because it is the second most abundant element on earth and there is already a mature industrial infrastructure in existence. However, it shows a large inherent volume change (400%) during insertion and extraction of lithium, which results in pulverization and fast capacity fading [2]. That is why silicon has not been commercialized as a practical anode material. To overcome this shortcoming, many different methods have been adopted for modification of the material such as utilization of nano-sized materials [3–9], surface coating of Si with various conducting materials [10–12], Si-based composites [13] and so on. These approaches have indeed improved the electrochemical performance of Si-based anodes but only to limited extent.

Recently, we have developed an approach to use Si nanotubes/nanowires with carbon-coating as negative electrode for Li-ion batteries [14,15]. Carbon-coated Si NWs electrodes were successfully synthesized with chemical vapor deposition method at first and then a thermal evaporation of carbon. Compared with the Si NWs without carbon-coating, the discharge capacity, cycle performance and rate capability of the carbon-coated Si NWs have been improved significantly. It could deliver a capacity of 3702 mAh g^{-1} and 3082 mAh g^{-1} in the first discharge/charge process when cycling between 0.02 V and 2.0 V (versus Li/Li^+) with a current density of 210 mA g^{-1}. The coulombic efficiency of the first cycle is 83.2%. The capacity still remains over 2150 mAh g^{-1} after 30 cycles. The carbon-coated Si NWs material also shows a good cycling performance at different current densities. The carbon-coated Si NWs show a better electrochemical performance than the pristine ones. It could be attributed to the carbon layer with a better electronic conductivity than the pristine material. However, carbon-coated material does not have satisfactory performance regarding both initial coulomb efficiency and capacity retention. That is why we have searched for a new coating layer having better conductivity than carbon and being able to suppress electrolyte decomposition on the surface of Si NWs. In this paper, we have prepared copper-coated Si NWs by a combination of chemical vapor deposition method and magnetron sputtering technique. The electrochemical performances of copper-coated Si NWs as an anode

* Corresponding author.
E-mail address: yyang@xmu.edu.cn (Y. Yang).

0378-7753/$ – see front matter © 2011 Elsevier B.V. All rights reserved.
doi:10.1016/j.jpowsour.2010.12.075

material were investigated in comparison with pristine and carbon-coated Si NWs.

2. Experimental

Si NWs were grown via a vapor–liquid–solid growth method. Stainless steel 304 (0.5 mm thick) substrates were decorated with a 10-nm-thick Au catalysts film by using ion sputtering technique. The substrate was then transferred into a CVD tube furnace. The gold thin film was annealed at 600 °C for 2 h under H_2 atmosphere, and subsequently Si NWs were grown at 540 °C with SiH_4 diluted in H_2 as precursor. The carbon-coated Si NWs were obtained by operation of carbon evaporation on the surface of the Si NWs. The copper-coated Si NWs was obtained by operation of magnetron sputtering on the surface of the Si NWs. The mass of the Si NWs, Si NWs with carbon-coating and copper-coating were accurately weighed by using a microbalance (Mettler Toledo XS3DU, 1 μg resolution) respectively. The electrode loading density in this study is about 0.6 mg cm^{-2}.

X-ray diffraction (XRD) patterns of the samples were obtained by a PANalytical X' Pert with Cu K_α radiation. The copper-coated Si NWs were analyzed by X-ray photoelectron spectroscopy (XPS) for the measurement of bonding energy. The XPS measurements were conducted with a PHI Quantum 2000 Scanning ESCA Microprobe equipped with an Al $K_{\alpha 1,2}$ X-ray radiation source. The spot size was about 200 μm. The survey scans were used a source with power and voltage of 35 W and 15 kV, respectively. Survey scans and high-resolution scans of the Si 2p, Cu 2p, O 1s, energy spectra were taken from each sample to identify the compounds present on the surface. The spectra were calibrated to the hydrocarbon peak at 284.5 eV. Morphology characterization was done by using scanning electron microscopy (Hitachi S4800) with a high sensitivity energy dispersive X-ray spectrometer (EDS) and transmission electron microscopy (Philips Tecnai F30, acceleration voltage 300 kV). A 300 kV Hitachi HD-2300A scanning transmission electron microscope (STEM) was also used.

The coin cells were assembled in an argon-filled glove box, using Li-metal foil as the negative electrodes, Si NWs (with and without carbon-coating) materials as cathode electrodes and 1 M $LiPF_6$/EC +DMC (1:1 in volume) as the electrolyte. The galvanostatic charge–discharge was carried out on a Land CT2001A cell tester at room temperature between 0.02 and 2.0 V (versus Li/Li^+). Cyclic voltammetry was performed on CHI608A, scanned from 2.0 to 0.01 V versus Li/Li^+ at a scan rate of 0.5 mV s^{-1}. The cells were also tested and evaluated by means of impedance spectroscopy. The explored frequency range was from 50 kHz to 100 mHz under AC stimulus with 10 mV of amplitude and no applied voltage bias. In the following results and discussion sections, we define that current rate 1 C is 4200 mA g^{-1}.

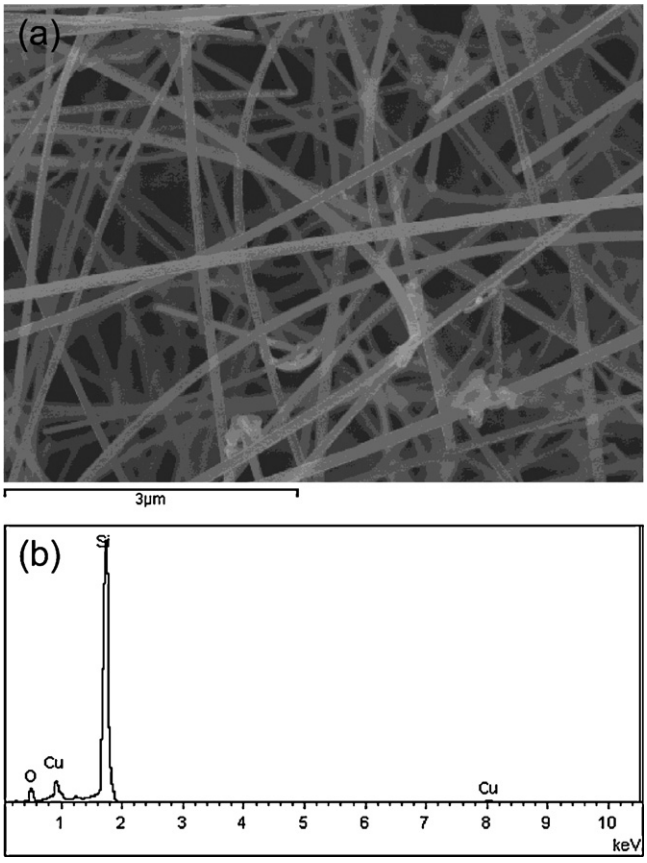

Fig. 1. (a) SEM image and (b) EDS spectrum of copper-coated Si NWs.

3. Results and discussion

3.1. Structure and morphology

Fig. 1 shows a SEM image of the copper-coated Si NWs. A large quantity of nanowires was obtained. The EDS analysis proves that the nanowires are composed of Si, a small amount of oxygen, which is attributed to the surface oxidation sheathing the nanowires, and also the copper.

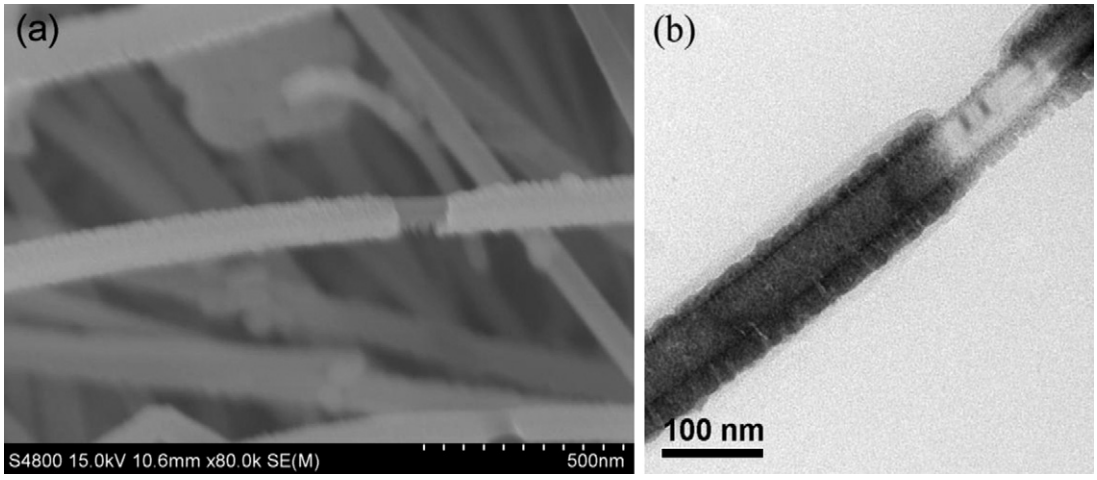

Fig. 2. (a) SEM and (b) TEM images of copper-coated Si NWs.

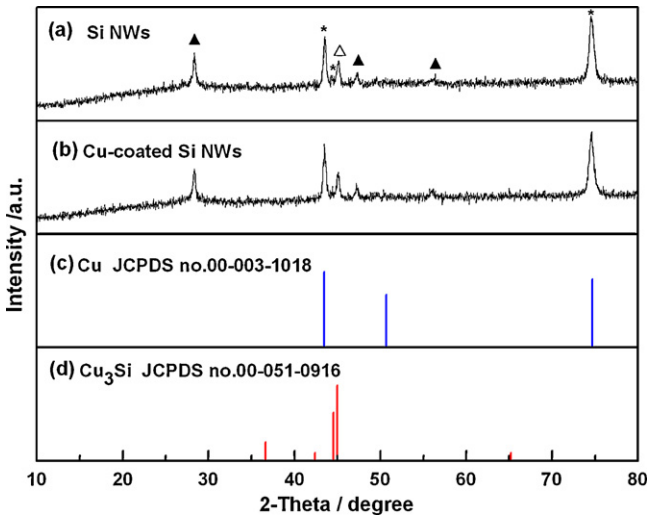

Fig. 3. XRD patterns of pristine (a) and copper-coated (b) Si NWs on stainless steel substrate. JCPDS files of copper (c) and (d) copper silicide ((*) from stainless steel, (△) from Fe_2Si, (▲) from Si NWs).

The SEM image shown in Fig. 2a reveals that the copper-coated Si NWs has a diameter of about 100 nm, and the Si NWs are coated by a surface layer. Fig. 2b shows the TEM image of the copper-coated Si NW materials magnified 29,500×. A layer is clearly displayed as a compact film on the surface of the Si NWs. The thickness of the copper-coating layer is about 10 nm. Normally, Si NWs grown via VLS (vapor–liquid–solid) mechanism show excellent crystallinity, although the surface may be covered by a thin layer of oxides [16,17].

In order to make sure whether copper or copper silicide is coated on the surface of Si NW, the XRD patterns of the Si NWs with and without copper-coating are compared. Fig. 3 shows the XRD patterns of pristine Si NWs (Fig. 3a), copper-coated Si NWs (Fig. 3b), copper and copper silicide (Cu_3Si) (Fig. 3c and d). As we can see, the X-ray diffraction (XRD) patterns of the pristine Si NWs and copper-coated Si NWs both show diffraction peaks associated with Si NWs, α-$FeSi_2$/Cu_3Si, and stainless steel (SS). Moreover there are no obvious changes in the 2θ position and no other impurities after coating. α-$FeSi_2$ may form at high temperature (540 °C) during Si NWs growth process [3,18]. Due to peak overlapping we were unable to distinguish copper silicide (Cu_3Si) and α-$FeSi_2$ on the Si NWs as well as copper and stainless steel from the XRD patterns only. A strong evidence to prove the existence of Cu_3Si is to compare Si XPS spectra of the different samples. As observed that in Fig. 4a, there is an obvious decline in the peak intensity of Si 2p core level spectra for copper-coated Si NWs. Moreover the Si 2p peak exhibits a small negative shift toward low binding energies. Fig. 4b shows a peak-fitting result for Cu-coated Si NWs. The overall peaks were fitted by the combination of respective binding energies (Cu_3Si: B.E. = 98.6 eV, Si: B.E. = 99.3 eV, SiO: B.E. = 100.0 eV, SiO_2: B.E. = 102.5 eV) for the different oxidation states of Si. In the literature, the 99.3 eV peak of Si 2p spectra is attributed to silicon [19]. Rossi et al. observed that Si 2p line shape exhibited a small shift toward low binding energies upon alloying copper [20–23]. Thus we think that the 98.6 eV peak of Si 2p spectra can be attributed to the formation of copper silicide (Cu_3Si). The other two types oxidation states of Si (B.E. = 100.0, 102.5 eV) were attributed to the presence of silicon oxides (SiO and SiO_2).

3.2. Electrochemical AC impedance

Fig. 5 shows the AC impedance spectra of the electrodes of Si NWs, Si NWs with carbon and copper-coating before cycling.

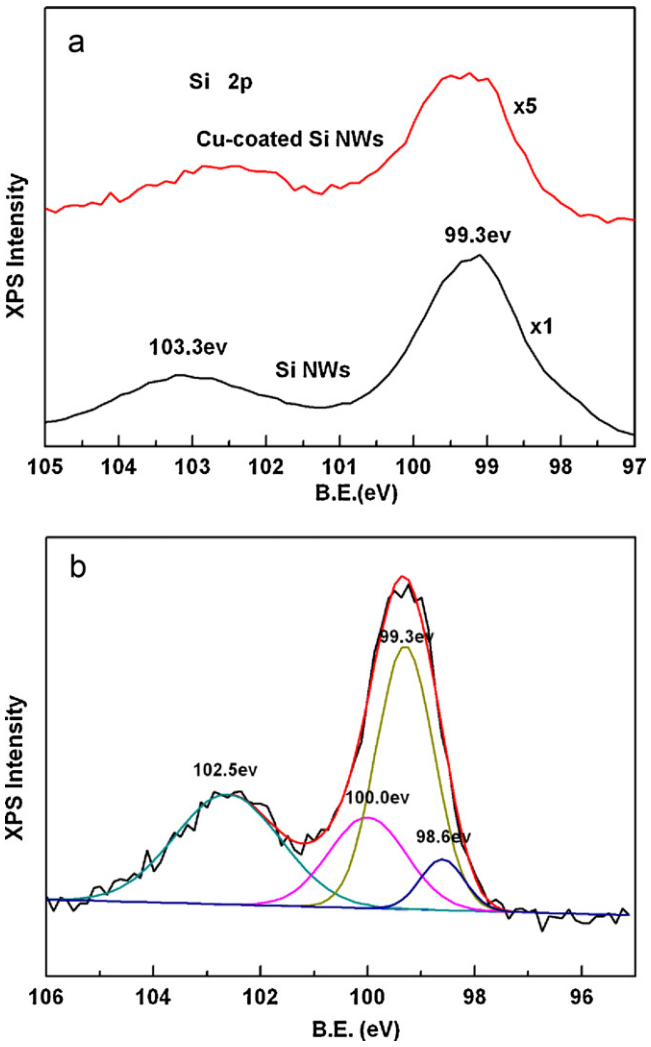

Fig. 4. (a) XPS spectra of pristine and copper-coated Si NWs. (b) Simulation of Si 2p core level spectra of the copper-coated Si NWs.

Both impedance spectra are composed of one semicircular arc at high frequency region, followed by a nearly vertical line against the real axis at low frequency region. These semicircular arcs can be assigned to charge transfer impedance of the electrodes. It is

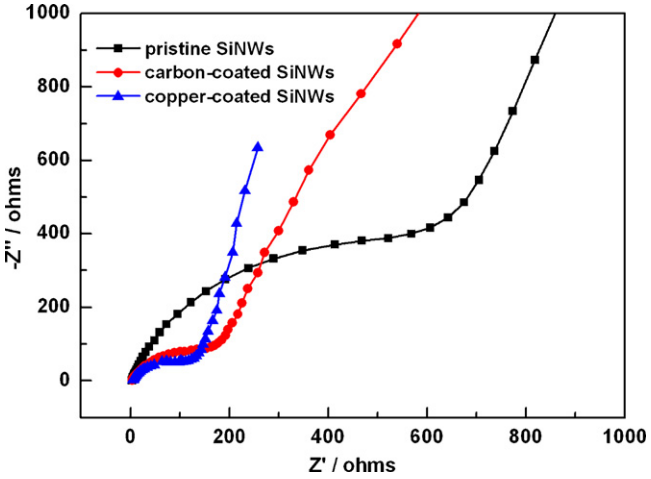

Fig. 5. AC impedance spectra of Si NWs electrode, Si NWs electrodes with carbon-coating and copper-coating before electrochemical cycling.

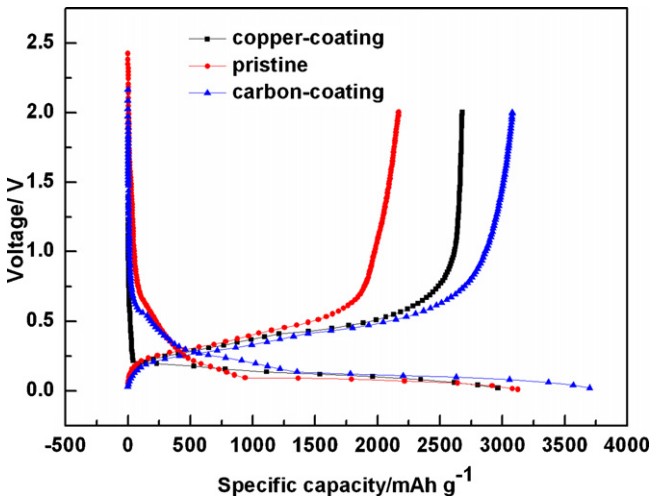

Fig. 6. Initial charge–discharge curves of the pristine Si NWs, Si NWs with carbon-coating and copper-coating at the rate of 0.05 C.

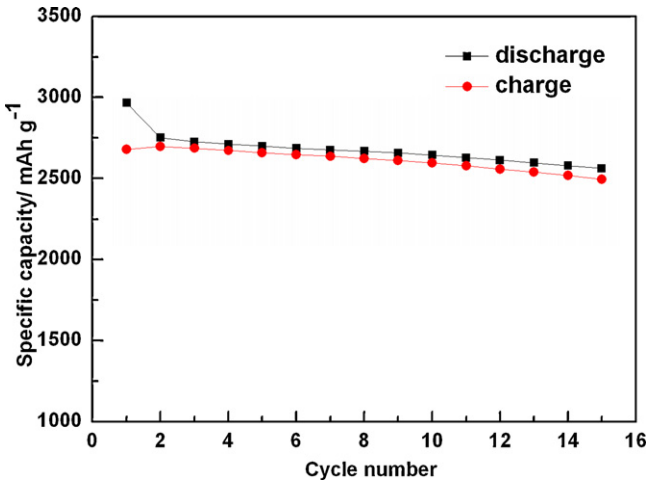

Fig. 7. Capacity as a function of cycle number for Si NWs with copper-coating at the rate of 0.05 C (1 C = 4200 mA g^{-1}).

clear that charge transfer resistances of these three materials are quite different, i.e. the resistance of the Si NWs is much larger than that of the copper-coated and carbon-coated Si NWs. Large differences in charge transfer resistance of the materials are attributed to the difference in the electrical conductivity of the materials. It is believed that the conductive coating layer such as copper and carbon enhance the electronic conductivity of the Si NWs greatly.

3.3. Initial charge–discharge performance

The first charge–discharge curves for Si NWs, Si NWs with carbon and copper coating in the range of 0.02 and 2.0 V at a current density of 210 mA g^{-1} are shown in Fig. 6. The first discharge capacity of the Si NWs material without any coating was 3125 mAh g^{-1}, while the charge capacity was 2171 mAh g^{-1}, indicating a coulombic efficiency of 69.5%. The first discharge capacity of the Si NWs with carbon-coating increases to 3702 mAh g^{-1}, while the charge capacity increases to 3082 mAh g^{-1}, giving a coulombic efficiency of 83.2%. Moreover, the first charge and discharge capacity of Si NWs with copper-coating are 2679 mAh g^{-1} and 2967 mAh g^{-1}, giving the highest coulombic efficiency of 90.3%. It should be noticed that the copper-coated Si NWs material delivers a lower charge–discharge capacity than that of the Si NWs with carbon-coating. The lower charge–discharge capacity of copper-coated Si NWs should be due to the less side reactions on Si surface after copper-coating. Moreover, some amount of the copper silicide formed also results in some capacity loss of Si NWs.

3.4. Cycling performance

Fig. 7 shows that discharge capacity of the Si NWs with copper-coating as a function of cycle numbers at the rate of 0.05 C. The discharge capacity of the Si NWs with copper-coating decreases gradually with cycles and 86.3% of its initial discharge capacity remains after 15 cycles at the rate of 0.05 C. For a comparison, we presented the data of discharge capacity retention of Si NWs with and without carbon-coating after 15cycles at the rate of 0.05 C in Table 1 which we have reported previously [14]. Obviously, the capacity retention of the copper-coated Si NWs is highest. The better cycling performance of copper-coated Si NWs may be due to the formation of copper and copper-alloy on Si NWs surface and they suppress the pulverization process of silicon materials during cycling process. In addition, better cycling performance of the copper-coated Si NWs may be attributed to the copper layer which has a better electronic conductivity than carbon and results in a lower polarization or a different SEI layer on the electrode surface.

In order to see the effects of volume changes of the Si NWs after charge–discharge cycling process, we have checked and compared the corresponding SEM images. As shown in Fig. 8, the copper-coated Si NWs cycling after 100 cycles at the rate of 0.5 C have an average diameter of about 120 nm (while the average diameter of pristine Si NWs after cycling is about 200 nm, see Fig. 8b) and their surfaces are quite smooth.

3.5. Rate capability

Fig. 9 shows the initial charge–discharge curves for the pristine Si NWs, Si NWs with carbon and copper coating at different rates of 0.05 C, 0.1 C and 0.5 C. We are able to observe that the ratios of initial discharge capacity at the rate of 0.5 C to the rate of 0.05 C are 73.6%, 86.5% and 103.2%, which corresponds to Si NWs, Si NWs with carbon and copper coating. It shows that the copper-coated Si NWs materials have a much better rate performance. We also investigated the cycling performances of the copper-coated Si NWs material at various current densities as presented in Fig. 10 and Table 2. The discharge capacity retentions are over 70% of their initial capacity after 30 cycles at different current densities. Apparently, the copper-coated Si NWs material shows a better cycling performance at various current densities as compared to Si NWs with and without carbon-coating.

For further comparison of cycling performances, the dependence of discharge capacity with cycle numbers for Si NWs with carbon and copper-coating at the rate of 0.5 C are showed in Fig. 11. As we can see, the discharge capacity of carbon-coated Si NWs maintains a value of 1504 mAh g^{-1}, giving a capacity retention ratio of 40.6% after 50 cycles while the copper-coated Si NWs maintains a value of 1750 mAh g^{-1}, giving a capacity retention ratio of 59.0% after 50 cycles. It is demonstrated clearly that improvement of the cyclic stability of the materials after copper-coating.

Table 1
The discharge capacity retentions of pristine Si NWs, Si NWs with carbon and copper coating after 15 cycles at the rate of 0.05 C.

Sample	1st (mAh g^{-1})	15th (mAh g^{-1})	Capacity retention (%)
Pristine Si NWs	3125	1992	63.7
Carbon-coated Si NWs	3702	2776	75.0
Copper-coated Si NWs	2967	2562	86.3

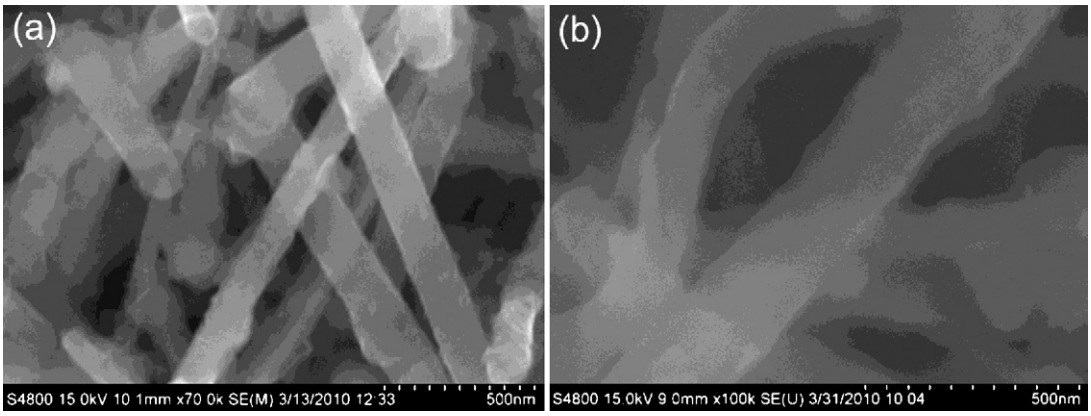

Fig. 8. SEM images of Si NWs (a) with and (b) without copper-coating after 100 cycles at the rate of 0.5 C.

Table 2
The discharge capacity retention of pristine Si NWs, Si NWs with carbon and copper coating after 30 cycles at different rates.

Sample	1st (mAh g^{-1})			30th (mAh g^{-1})			Capacity retention %		
	0.05 C	0.1 C	0.5 C	0.05 C	0.1 C	0.5 C	0.05 C	0.1 C	0.5 C
Pristine Si NWs	3125	2497	2299	1582	1493	1360	50.6	59.8	59.1
Carbon-coated Si NWs	3702	3543	3201	2180	2094	2169	58.9	59.1	67.8
Copper-coated Si NWs	2967	2917	3061	2138	2050	2216	72.0	70.3	72.4

3.6. Cyclic voltammetry (CV)

Cyclic voltammetry curves of Si NWs with copper-coating in the potential range of 0.01 and 2.0 V (versus Li/Li^+) at a scan rate of 0.5 mV s^{-1} is shown in Fig. 12. For the cyclic voltammetry curves of the copper-coated Si NWs, a current peak associated with the insertion of lithium ion into the copper-coated Si NWs begins at the potential of about 200 mV and becomes quite large below 100 mV in the first negative sweeping process. In the first positive sweeping, the current peaks appear at about 370 and 510 mV, is corresponding to the extraction of lithium ion from the copper-coated Si NWs. The increasing magnitude of the current peaks in following cycles may be due to the gradual electrochemical activation of the electrode during the scanning process [5]. There are no apparent current peaks related to SEI [3] layer formation in the potential range of

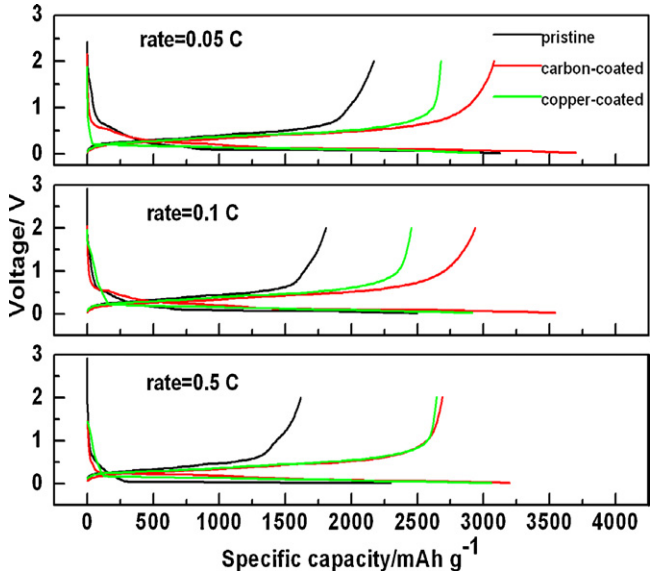

Fig. 9. Initial charge–discharge curves for the pristine Si NWs, Si NWs with carbon-coating and copper-coating at the rate of 0.05, 0.1, 0.5 C.

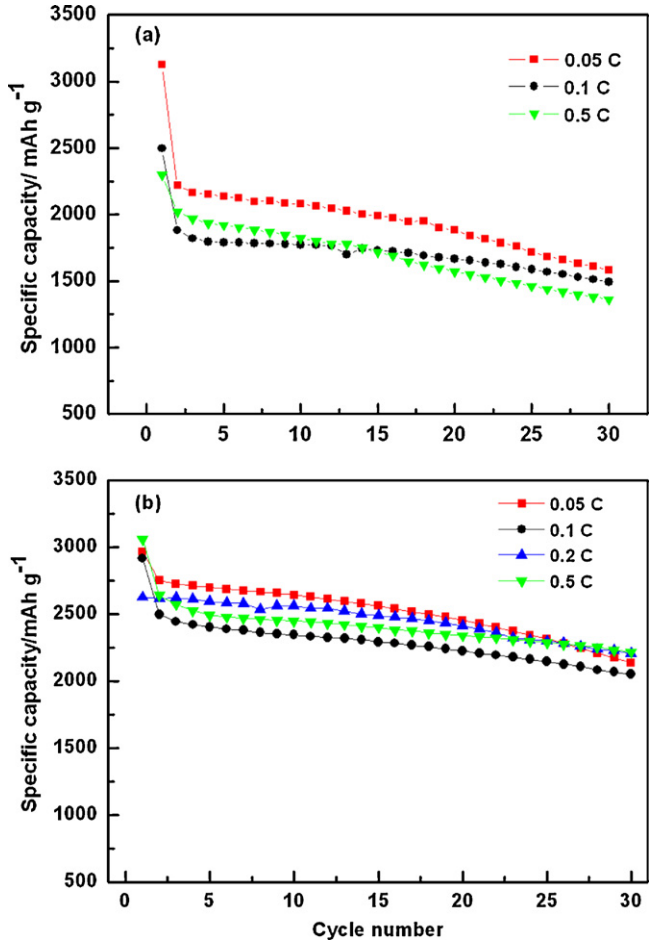

Fig. 10. Capacity–cycle number curves for Si NWs without (a) and with (b) copper-coating at different rates.

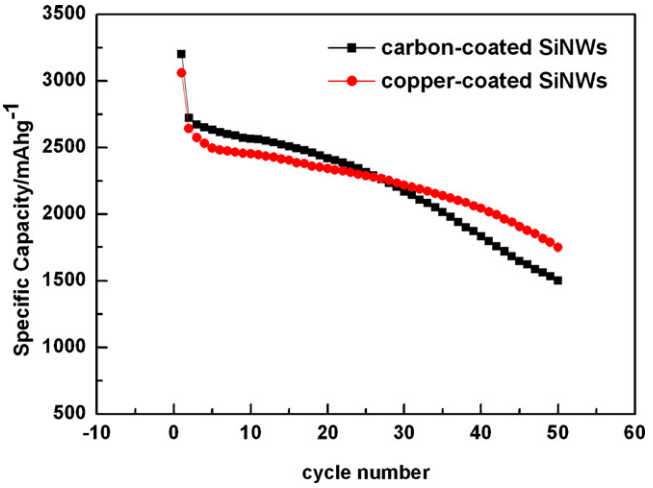

Fig. 11. Capacity–cycle number curves for Si NWs with carbon-coating and copper-coating at the rate of 0.5 C.

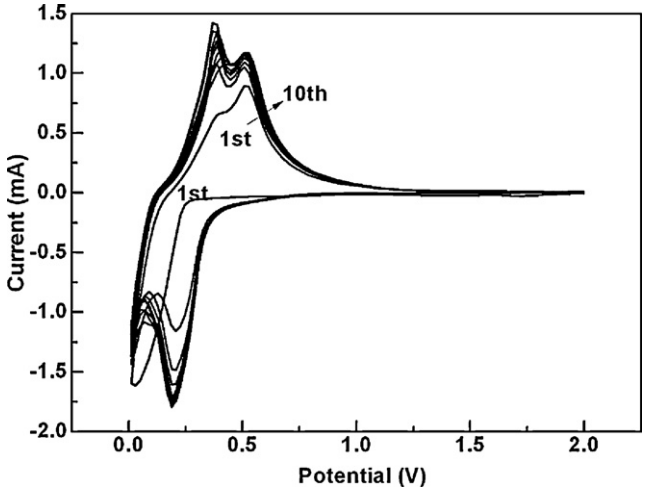

Fig. 12. Cyclic voltammetry of the Si NWs with copper-coating between 0.01 V and 2.0 V (versus Li/Li^+) at a scan rate of 0.5 mV s^{-1}.

0.5 V and 0.7 V during the first scanning process. In addition, the relative low capacity loss of copper-coated Si NWs contributing to the initial irreversible capacity in the first cycle would be smaller than pristine Si NWs according to our results.

4. Conclusion

The copper-coated Si NWs electrodes exhibit higher initial coulombic efficiency, better cycling stability and rate capability than Si NWs with and without carbon-coating. Initial coulombic efficiency of Si NWs with copper-coating is 90.3% in the voltage range of 0.02 and 2.0 V at a current density of 210 mA g^{-1}. The initial discharge capacity of the Si NWs with copper-coating decreases gradually during charge–discharge cycling and 86.3% of its initial discharge capacity remains after 15 cycles at 0.05 C rate. The ratios of initial discharge capacity at the rate of 0.5 C to the rate of 0.05 C is 103.2% corresponding to Si NWs with copper-coating, revealing a good rate capability; The cycling performances of the copper-coated Si NWs material at various current densities were investigated, the results showed that the discharge capacity retention ratios of copper-coated Si NWs material is over 70% of its initial capacity after 30 cycles at different current densities. It also proved that the copper-coated Si NWs material showed a better cycling performance compared with pristine and carbon-coated Si NWs.

The presence of copper silicon alloy layer can improve the electrochemical performance of the Si NWs, and the reason may be that it can suppress the reductive decomposition of the electrolyte solution on the surface and pulverization of silicon materials generated from volume changes during large amount of insertion and extraction of lithium. Moreover, the copper and copper silicon alloy formed has a higher conductivity than that of silicon, so the distribution of the electric field becomes more well proportioned, which can depress the cross potential aroused by polarization. Nevertheless, the thickness and homogeneity of Cu coating layer have some effects on the electrochemical performance of Si NWs, i.e. if some of the SiNWs are not coated by Cu or the Cu layers are very thin. In such a case the pulverization of Si easily occurs, which lead to the decrease of the capacity during cycling. The increased of Cu coating can further improve the cyclic stability while the capacity decreases. These effects will be investigated in the future study.

Acknowledgments

This work was financially supported by National Natural Science Foundation of China (no. 90606015), and the National Basic Research Program of China (973 program, grant no. 2007CB209702).

References

[1] C.J. Wen, R.A. Huggins, J. Solid State Chem. 37 (1981) 271–278.
[2] B.A. Boukamp, G.C. Lesh, R.A. Huggins, J. Electrochem. Soc. 128 (1981) 725–729.
[3] C.K. Chan, H.L. Peng, G. Liu, K. McIlwrath, X.F. Zhang, R.A. Huggins, Y. Cui, Nat Nanotechnol. 3 (2008) 31–35.
[4] U. Kasavajjula, C.S. Wang, A.J. Appleby, J. Power Sources 163 (2007) 1003–1039.
[5] M. Green, E. Fielder, B. Scrosati, M. Wachtler, J.S. Moreno, Electrochem. Solid-State Lett. 6 (2003) A75–A79.
[6] H. Li, X.J. Huang, L.Q. Chen, G.W. Zhou, Z. Zhang, D.P. Yu, Y.J. Mo, N. Pei, Solid State Ionics 135 (2000) 181–191.
[7] X.W. Zhang, P.K. Patil, C.S. Wang, A.J. Appleby, F.E. Little, D.L. Cocke, J. Power Sources 125 (2004) 206–213.
[8] W.R. Liu, Z.Z. Guo, W.S. Young, D.T. Shieh, H.C. Wu, M.H. Yang, N.L. Wu, J. Power Sources 140 (2005) 139–144.
[9] T. Zhang, J. Gao, H.P. Zhang, L.C. Yang, Y.P. Wu, H.Q. Wu, Electrochem. Commun. 9 (2007) 886–890.
[10] J.W. Kim, J.H. Ryu, K.T. Lee, S.M. Oh, J. Power Sources 147 (2005) 227–233.
[11] M. Yoshio, H. Wang, K. Fukuda, T. Umeno, N. Dimov, Z. Ogumi, J. Electrochem. Soc. 149 (2002) A1598–A1603.
[12] W.R. Liu, J.H. Wang, H.C. Wu, D.T. Shieh, M.H. Yang, N.L. Wu, J. Electrochem. Soc. 152 (2005) A1719–A1725.
[13] M. Yoshio, S. Kugino, N. Dimov, J. Power Sources 153 (2006) 375–379.
[14] H.X. Chen, Z.X. Dong, Y.P. Fu, Y. Yang, J. Solid State Electrochem. 14 (2010) 1829–1834.
[15] Y.P. Fu, H.X. Chen, Y. Yang, Electrochemistry 15 (2009) 56–61 (Chinese).
[16] N. Wang, Y.H. Tang, Y.F. Zhang, C.S. Lee, I. Bello, S.T. Lee, Chem. Phys. Lett. 299 (1999) 237–242.
[17] Y. Wu, Y. Cui, L. Huynh, C.J. Barrelet, D.C. Bell, C.M. Lieber, Nano Lett. 4 (2004) 433–436.
[18] A. Netz, R.A. Huggins, W. Weppner, J. Power Sources 119–121 (2003) 95–100.
[19] J. Chastain, R.C. King Jr., Handbook of X-ray Photoelectron Spectroscopy, Physical Electronics Inc., Minnesota, 1995.
[20] G. Rossi, I. Kendelewicz, I. Lindau, W.E. Spicer, J. Vac. Sci. Technol. A 1 (1983) 987–990.
[21] I. Abbati, M. Grioni, J. Vac. Sci. Technol. 19 (1981) 631–635.
[22] F. Ringeisen, J. Derrien, E. Daugy, J.M. Layet, P. Mathiez, F. Salvan, J. Vac. Sci. Technol. B 1 (1983) 546–552.
[23] I.C. Kim, D. Byun, S. Lee, J.K. Lee, Electrochim. Acta 52 (2006) 1532–1537.